Diabetes Research and Clinical Practice, 6 (1989) 279–296
Elsevier

DRC 00279

Diabetic and hypoglycemic neuropathy — a comparison in the BB rat

Anders A.F. Sima, Wei-Xian Zhang* and Douglas A. Greene[1]

Neuropathology Research Laboratory, Department of Pathology, University of Manitoba, Winnipeg, MB, Canada, and [1]Diabetes Research and Training Center, University of Michigan, Ann Arbor, MI, U.S.A.

(Received 25 October 1988, accepted 1 December 1988)

Key words: Diabetes; Hypoglycemia; Insulin; Peripheral neuropathy; BB rat

Summary

Functional and structural neuropathy was examined in hyperglycemic (diabetic) BB rats maintained on small maintenance doses of insulin, hyperglycemic BB rats receiving no insulin, and BB rats in whom hypoglycemia was induced by the administration of excessive insulin doses. The data were compared with those of non-diabetic age- and sex-matched BB rats. Functional deficits and structural abnormalities were comparable in diabetic rats with and without insulin supplementation, suggesting that the generally necessary insulin dosing in this model does not per se account for the neuropathy. Hypoglycemic neuropathy was characterized by slowing of nerve conduction velocity, marked loss of anterior horn motoneurons and Wallerian degeneration, as well as loss of large myelinated fibers, suggesting a neuropathy involving predominantly motoneurons. Diabetic neuropathy was not associated with nerve cell loss but showed marked axonal atrophy involving predominantly sensory fibers. Thus, diabetic and hypoglycemic neuropathies are two distinguishable entities under strict experimental conditions, but may overlap in human diabetic subjects in whom tight insulin control is desirable.

Address for correspondence: Dr. Anders A.F. Sima, Neuropathology Research Laboratory, Department of Pathology, University of Manitoba, 770 Bannatyne Avenue, Winnipeg, MB, R3E 0W3, Canada.

*Dr. Zhang is a visiting scientist from the Medical University of Shanghai, Peoples Republic of China, supported by ICI-Americas, Wilmington, DE, U.S.A.

Introduction

Diabetic neuropathy in human subjects is associated with impaired nerve conduction velocity and a spectrum of structural changes that include axonal degeneration, paranodal demyelination and loss of

0168-8227/89/$03.50 © 1989 Elsevier Science Publishers B.V. (Biomedical Division)

myelinated nerve fibers, as well as endoneurial ischemic damage [1–9].

The spontaneously diabetic BB rat is an authentic model of human insulin-dependent diabetes mellitus (IDDM) and as such develops the whole spectrum of functional and structural changes seen in human diabetic neuropathy including nerve fiber loss and endoneurial ischemic lesions. We have previously used this model extensively to investigate the nature of underlying metabolic and functional abnormalities in diabetic peripheral nerve and to correlate these changes with the development of subsequent structural abnormalities [10–20]. In brief, these studies have suggested that the initial metabolic defect, involving an activated polyol pathway, decreased *myo*-inositol content and impaired activity of (Na,K)-ATPase, via a protein kinase C defect, is a consequence of hyperglycemia, and precedes and conditions the development of structural diabetic neuropathy [10,21 23]. The nerve conduction slowing in the BB rat has been attributed to alterations in nerve Na and Na-related metabolism, secondary to impaired (Na,K)-ATPase activity, resulting in a selective nerve conduction block of large and rapidly conducting myelinated nerve fibers [11–13]. Accompanying histologically demonstrated paranodal nerve fiber swelling has been associated with a fivefold elevation of intra-axonal Na concentration [12]. These metabolic, electrophysiological and structural abnormalities are completely reversed by vigorous insulin treatment within the first 6 weeks of diabetes [10,13].

A countervailing opinion, however, holds that the degeneration of peripheral nerve seen in the diabetic BB rat may be a complication of insulin treatment rather than a manifestation of diabetes [24,25], since the diabetic BB rat generally requires small daily maintenance doses of insulin for its survival [26,27]. However, a small percentage of diabetic BB rats can be maintained at substantial hyperglycemic levels for prolonged periods of time without exogenous insulin supplementation, probably due to an incomplete immune-mediated destruction of insulin secreting β cells [26,27].

To assess the role of even small doses of exogenous insulin in the development of diabetic polyneuropathy in the BB rat, we compared functional and structural peripheral nerve abnormalities in diabetic BB rats receiving small daily insulin injections, and those maintained at identical hyperglycemic levels without exogenous insulin supplementation. The nerve conduction and morphometric data obtained from these two diabetic groups were compared with those obtained from BB rats rendered hypoglycemic following excessive exogenous insulin administration, since previously reported abnormalities in insulin-treated diabetic rats [24,25] could represent hypoglycemic nerve damage.

Material and methods

Animals

Prediabetic male BB rats and age-matched non-diabetes-prone male BB rats were obtained from the Department of Pathology, University of Massachusetts, Worchester, MA (courtesy of Dr. A.A. Like) and maintained in individual air-filtered metabolic cages with ad libitum access to water and rat chow (Wayne Lab. Blox F-6, Wayne Laboratory Animal Diets, Wayne Feed Div., Winnipeg, MB, Canada). Body weight, urine volume, glucosuria and ketonuria (Test Tape, Eli Lilly Canada Inc., Toronto, Ont., Canada) were monitored daily, and blood glucose was measured in tail-vein blood samples by Ames Eyetone (Miles Laboratory, Ltd., Rexdale, Ont., Canada) every week, as previously described in detail [18,22].

Diabetic animals (DI and DII)

One group of five diabetic BB rats was treated with small daily doses of protamine zink insulin (PZI) (0.5–3.0 U/day) from onset of diabetes at 3 months of age to 9 months of age (DI). They were maintained hyperglycemic at blood glucose levels greater than 17 mmol/l. A second group of four diabetic BB rats was maintained at hyperglycemic levels greater than 17 mmol/l from onset of diabetes at 3 months of age to 9 months of age without ever having received exogenous insulin supplementation (DII).

Hypoglycemic animals (HI and HII)
In eight non-diabetic BB rats, age 8.5 months, *hypo*glycemia was induced by four daily injections of PZI (0.5–4.0 U/day) in order to achieve and maintain blood glucose levels at less than 3.0 mmol/l for 6 days. Four animals were killed after 6 days of excessive insulin treatment (HI), and four animals were left untreated for an additional 7 days before sacrifice (HII).

Controls (C)
A group of seven non-diabetic age- and sex-matched BB rats was used as non-diabetic controls (C) and killed at 9 months of age.

Electrophysiological studies
The day before sacrifice, animals were lightly anesthetized with ethyl ether (Fisher Scientific Co., Fair Lawn, NJ). Motor nerve conduction velocity (MNCV) was determined non-invasively in the sciatic-posterior tibial nerves in a temperature-controlled environment as previously described in detail [28]. The left sciatic-tibial conducting system was stimulated proximally at the sciatic notch and distally at the ankle via bipolar electrodes using supramaximal stimuli (8 V) from a Tektronix TM 501 stimulator (Tektronix Inc., Beaverton, OR). Evoked muscle potentials were collected from the first interosseous space of the hind paw by a unipolar platinum recording electrode and displayed on a Tektronix 511 storage oscilloscope. MNCV was calculated by subtracting the distal from the proximal latency measured in ms from stimulus artifact to take-off of the evoked muscle potential. The difference was divided into the distance between the stimulating electrodes measured in mm, yielding a value for nerve conduction velocity in m/s.

Tissue collection
Animals were anesthetized with sodium phenobarbital (50 mg/kg body weight; i.p.) and killed by whole body perfusion with a 0.05 M cacodylate-buffered (pH 7.4) 2.5% glutaraldehyde fixative, which for hyperglycemic animals was adjusted to an osmolality of 500 mosmol with sucrose to achieve serum iso-osmolality. The right sural and tibial nerves, the right spinal ganglion of L5 as well as the L5 segment of the spinal cord were dissected and immersed in the same fixative for 3–4 h at 4°C. The specimens were post-fixed in cacodylate-buffered 1% osmium tetroxide (pH 7.4) for 2 h at 4°C, and dehydrated through an ascending series of ethanol. The proximal 3–4 mm of the sural and tibial nerves were used for teased fiber preparations in Epon [16]. The remaining sural and tibial nerves as well as spinal cord segments were embedded in Epon. Semithin sections were used for light microscopic examination and ultra-thin sections were stained with aqueous uranyl acetate and lead citrate for electron microscopic examination.

Quantitative morphometry

Myelinated fiber size, distribution, density and occupancy in sural and tibial nerves. Semi-thin (0.5 μm) toluidine-blue stained transverse sections of the entire unifascicular mainly sensory sural and mixed sensory-motor tibial nerve were photographed, and prints with a magnification of 1000 times were used to calculate the area of each myelinated fiber with the aid of a 9874 A digitizer interfaced with a 9825A desk computer and plotter (Hewlett-Packard Co., Cupertino, CA). Composite histograms were compiled for each animal group, in which each fiber size frequency is expressed as a percentage of total fibers, as previously described in detail [16]. The fascicular area of each nerve was digitized from photographic prints with a total magnification of 250 times. Myelinated fiber density per unit area and myelinated fiber occupancy (percent of the fascicular area occupied by myelinated fibers) were calculated as previously described [16].

Axon–myelin ratio. Electron microscopic prints with a total magnification of 20,790 times were used to calculate the ratio between the axonal area (μm^2) and the corresponding myelin sheath thickness expressed by the number of myelin lamellae [16]. A mean of 44.3 ± 2.7 systematic randomly chosen fibers from each nerve were examined.

Density of anterior horn cells and dorsal root ganglion cells. The number of α motoneurons of the anterolateral anterior horn and of dorsal root ganglion cells of the L5 segment was calculated from photographic prints at a total magnification of 500 times obtained from semi-thin (0.5 μm) toluidine-blue stained sections. From each tissue block four sections were examined 30 μm apart. Neurons were counted and the areas of neuropil occupied by motoneurons and ganglion cells were digitized yielding nerve cell densities (n/mm^2). A split cell error correction factor of 0.542 was used for both α motoneurons and dorsal root ganglion cells [29].

Teased fiber analysis of sural and tibial nerves. The spectrum of abnormal myelinated fibers was assessed by analysis of teased fibers. A mean of 63 ± 5 randomly teased single fibers from each nerve was examined light microscopically at a magnification of 480 times. Each fiber was assigned to one of eight categories based on characteristic structural features according to a modification [9] of the technique described by Dyck et al. [8]: (A) normal fibers; (B) paranodal swelling defined as a paranodal diameter > 150% of the internodal diameter; (C) paranodal demyelination; (D) excessive myelin wrinkling; (E) intercalated (remyelinated) nodes; (F) Wallerian degeneration; (G) segmental demyelination; (H) regenerated and/or remyelinated fibers. The frequencies of abnormalities were expressed as a percentage of fibers examined.

Statistical analysis

The results are presented as mean ± SEM, and significance of difference was calculated using ANOVA followed by modified *t*-test. Linear regression analysis was performed by the method of least squares. The comparison of myelinated fiber size distributions was performed using chi-square distribution, and the individual size frequencies were compared using Student's *t*-test.

Results

Clinical observation

Prediabetic rats ($n = 9$) developed diabetes at 94 ± 8 days of age and were persistently hyperglycemic for 182 ± 9 days. At time of sacrifice diabetic rats receiving small maintenance doses of insulin (DI) and those receiving no exogenous insulin (DII) showed similar degrees of hyperglycemia (Table 1). Diabetic rats (DI and DII) demonstrated a significant ($P < 0.001$) reduction in body weight gain as well as a 26% slowing of MNCV (Table 1). Hypoglycemic animals were never rendered comatose and after 1 week of excessive insulin treatment showed blood glucose levels of approximately half the normal control value (Table 1). One group killed immediately after 6 days of excessive insulin treatment (HI) showed no significant body weight loss, whereas animals maintained for an additional week (HII) demonstrated an 18% ($P < 0.05$) weight loss (Table 1). MNCV in hypoglycemic animals was 19% slower than in age-matched controls (Table 1). Hyperglycemic BB rats exhibited no gross neurological deficits, whereas rats in whom hypoglycemia was induced revealed after 3–4 days of insulin injection weakness of the extremities, particularly pronounced in the hind legs. This weakness disappeared 4–5 days after insulin injections were discontinued in the HII group, except for one animal who showed persistent weakness.

Quantitative morphology in sural nerve

Hypoglycemic animals (HI and HII). Insulin-induced hypoglycemia resulted in significant shifts in sural nerve fiber caliber spectra toward smaller fibers as compared with non-diabetic controls ($P < 0.001$) due to a decrease in the frequencies of large myelinated fibers (Fig. 1a). The loss of large myelinated fiber sizes in hypoglycemic rats was also reflected in a significant ($P < 0.0001$) reduction in

TABLE I

CLINICAL DATA AT TIME OF SACRIFICE

	Age (months)	Weight (g)	Insulin (U/day)	Blood glucose (mmol/l)	MNCV (m/s)
Control (C) (n = 7)	9	553 ± 18	0	4.5 ± 0.8	54.7 ± 1.1
		$P<0.001$		$P<0.001$	$P<0.001$
Diabetic (DI) (n = 5)	9 (6 m diab)	382 ± 12	0.5–3.5	20.8 ± 2.1	40.6 ± 0.8
		$P<0.05$		$P<0.05$	$P<0.05$
Diabetic (DII) (n = 4)	9 (6 m diab)	318 ± 44	0	23.4 ± 1.0	40.4 ± 1.4
		$P<0.01$		$P<0.001$	
Hypoglycemic (HI) (n = 4)	6	503 ± 17	0.5–4.0	2.4 ± 0.2	44.2 ± 1.0
Hypoglycemic (HII) (n=4)	6	451 ± 32	0.5–4.0	2.0 ± 0.1*	43.4 ± 1.2

Comparisons of body weight, daily insulin dose, blood glucose levels and motor nerve conduction velocities in hyperglycemic animals with (DI) and without (DII) insulin supplementation and hypoglycemic animals immediately after 6 days of insulin-induced hypoglycemia (HI) and 7 days following 6 days of insulin-induced hypoglycemia (HII). The values (mean ± SEM) are compared with those obtained from non-diabetes-prone euglycemic control rats.

* Blood glucose values reflect those at termination of insulin treatment.

mean myelinated fiber size (Table 2). Myelinated fiber density was moderately ($P < 0.02$) increased in acutely hypoglycemic rats (HI) while fiber occupancy was unchanged when compared with non-diabetic controls (Table 2), probably reflecting a significant ($P < 0.001$) increase in regenerating sural nerve fibers (see column H, Table 3 and below). Hypoglycemic animals who were allowed to survive for an additional week (HII) showed a similar reduction in mean fiber size (Table 2), whereas fiber density was normalized and fiber occupancy was decreased to 61% of normal (Table 2), in keeping with loss of large myelinated fibers and the addition of small regenerating fibers. The axon–myelin ratios (regression coefficients b in Fig. 2a) were significantly decreased in both hypoglycemic groups ($P < 0.001$) (HI and HII in Fig. 2a) compared with non-diabetic control rats (C in Fig. 2a), suggesting that axonal atrophy may, in addition to loss of large myelinated fibers, have accounted for the decrease in myelinated fiber size in hypoglycemic rats.

Hyperglycemic animals (DI and DII). Similar to hypoglycemic animals diabetic rats showed highly significant shifts ($P < 0.001$) of myelinated fiber caliber spectra toward smaller fiber sizes (Fig. 1b). These shifts in caliber size distribution were due to a simultaneous decrease in the frequencies of large myelinated fibers and an increase in the frequencies of small myelinated fibers (Fig. 1b). The fiber size distribution in diabetic rats maintained on small doses of insulin (DI) was not markedly different from that in diabetic rats maintained on no insulin (Fig. 1c). Mean myelinated fiber size was significantly reduced ($P < 0.0001$) in both diabetic groups (Table 2). Myelinated fiber densities were increased

with approximately 15% in both groups, whereas fiber occupancies showed no significant change (Table 2), in keeping with shrinkage of the endoneurial space and a substantial atrophy of myelinated fibers as previously reported [16]. Axon–myelin ratios in both diabetic groups revealed similar and significant decreases ($P < 0.001$) (DI and DII in Fig. 2a) compared with non-diabetic control rats (C in Fig. 2a), suggesting that axonal atrophy may account for myelinated fiber atrophy. Axon–myelin ratios in

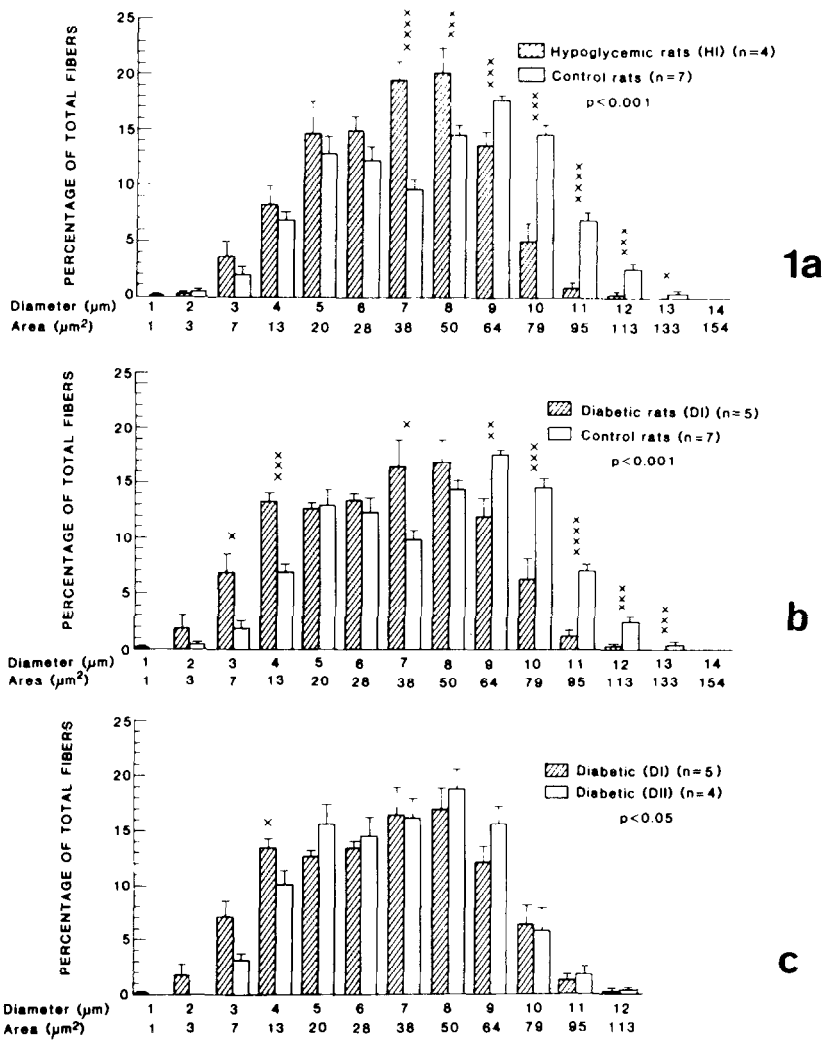

Fig. 1. Myelinated fiber areas were measured from photographic prints, taken from toluidine blue cross-sections of the unifascicular sural nerve and magnified 1000 times. Histograms were constructed, in which each fiber size frequency is expressed as a percentage of total fibers. The fiber size distributions are compared using chi-square distribution and significance of difference is indicated in a, b and c. (a) Hypoglycemic rats killed immediately following a 6-day period of excessive insulin injections (HI) are compard with age- and sex-matched control rats (C). The frequencies of large myelinated fibers are markedly decreased, indicating loss of large myelinated fibers. (b) Myelinated fiber caliber spectra of diabetic rats treated with small maintenance doses of insulin (DI) and control rats (C) are compared. In diabetic rats the frequencies of large fibers are decreased, while those of small fibers are increased, suggesting a generalized atrophy of fibers. (c) Myelinated fiber size frequencies of diabetic rats with insulin supplementation (DI) are compared with those of diabetic rats who never received exogenous insulin (DII). No major differences are demonstrated in myelinated fiber size distribution between the two diabetic groups. ×, $P < 0.05$; ××, $P < 0.02$; ×××, $P < 0.01$; ××××, $P < 0.001$.

TABLE 2

NUMERICAL MORPHOMETRIC DATA OF SURAL NERVES

	Mean fiber size (μm)	Fiber density (fibers/mm)	Fiber occupancy (%)
	***	*	**
Control (C) (n = 7)	49.4 ± 1.0	11671 ± 444	57.5 ± 1.9
	$P<0.0001$	$P<0.05$	
Diabetic (DI) (n = 5)	35.7 ± 1.7	13794 ± 383	49.4 ± 2.9
		$P<0.02$	$P<0.0001$
Diabetic (DII) (n = 4)	38.7 ± 2.0	13423 ± 396	51.7 ± 1.5
		$P<0.02$	$P<0.01$
Hypoglycemic (HI) (n = 4)	38.2 ± 1.3	14300 ± 932	54.6 ± 3.8
			$P<0.005$
		$P<0.005$	$P<0.001$
Hypoglycemic (HII) (n = 4)	35.5 ± 2.0	10082 ± 1748	35.2 ± 5.8

Comparison of mean myelinated fiber size, myelinated fiber density and occupancy (endoneurial area occupied by myelinated fibers) between the various experimental groups. Values are expressed as mean ± SEM.

*** ANOVA $P<0.0001$.

** ANOVA $P<0.001$.

* ANOVA $P<0.02$.

diabetic rats were not different from those calculated from sural nerves of hypoglycemic animals (Fig. 2a).

Teased fiber analysis of sural nerve

Hypoglycemic animals (HI and HII). Excessive insulin treatment resulted in a marked decrease in the frequencies of normal fibers in the HI group to 48% of total fibers and an additional significant ($P < 0.0001$) decrease to 30% in rats allowed to survive the hypoglycemic 6-day period for another 7 days (Table 3). This decrease was to a large extent accounted for by significant increases in the frequencies of fibers exhibiting Wallerian degeneration, which increased from 13% in the HI group to 38% in the HII group (Table 3), as well as marked ($P < 0.005$) increases in the frequencies of fibers exhibiting excessive myelin wrinkling (approximately 15% in both groups). Other abnormalities which were demonstrated in single teased fibers included paranodal swelling, paranodal demyelination, intercalated nodes, and segmental demyelination which were all increased compared with nondiabetic control rats (Table 3).

Hyperglycemic animals (DI and DII). The frequencies of normal fibers were reduced in both hyperglycemic groups ($P < 0.0002$) compared to nondiabetic control rats with no intergroup difference (Table 3). Nevertheless, normal fibers were still demonstrated approximately twice as frequently in

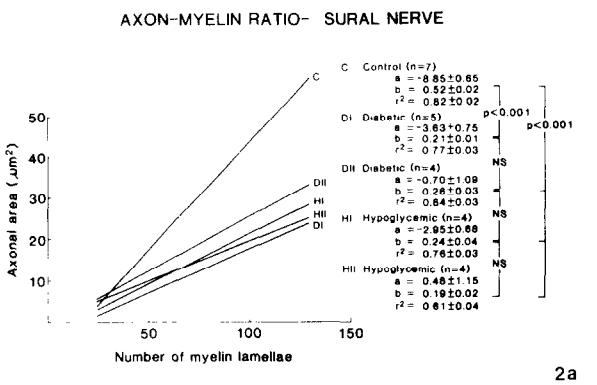

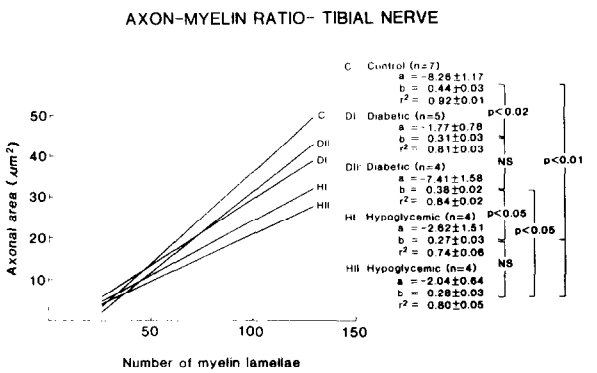

Fig. 2. Axon–myelin ratio was calculated from measurements of axonal area and the thickness of the corresponding myelin sheath, expressed as the number of myelin lamellae. The slopes of the linear regressions (b in the equation $y = a + bx$) obtained from each nerve were compared between groups. (a) Intergroup comparisons of the sural nerve axon–myelin ratios. Both diabetic groups (DI and DII) as well as both hypoglycemic groups (HI and HII) are significantly decreased compared with age- and sex-matched control rats (C). The decrease in axon–myelin ratio, indicating axonal atrophy, was similar in diabetic and hypoglycemic rats and did not differ between the two diabetic (DI and DII) or the two hypoglycemic groups (HI and HII). (b) The same comparisons are made between axon–myelin ratios in the tibial nerve. The axon–myelin ratio was only marginally decreased in diabetic rats, reaching significance in diabetic rats treated continuously with insulin (DI), when compared with control rats (C). Hypoglycemic rats (HI and HII) showed a slightly more severe decrease in their axon–myelin ratios compared with control rats (C), and they were significantly ($P < 0.05$) lower when compared with non-insulin-treated diabetic rats (DII).

hyperglycemic rats as in hypoglycemic animals (Table 3). The most commonly encountered abnormality in diabetic nerves was excessive myelin wrinkling (Table 3) which reflects axonal atrophy [9]. Myelin wrinkling was slightly more common in non-insulin-treated diabetic rats (Table 3), while still approximately half as frequent as in rats with induced hypoglycemia. Other previously described abnormalities in teased myelinated fibers of the diabetic BB rat included paranodal swelling and demyelination, intercalated nodes, segmental demyelination, as well as regenerating fibers (Table 3). Paranodal swelling was significantly ($P < 0.002$) more frequent in diabetic rats compared with hypoglycemic animals (HII), whereas paranodal demyelination occurred with similar frequencies in diabetic and hypoglycemic rats. In contrast, intercalated nodes, segmental demyelination and regenerating fibers tended to be more frequent in hypoglycemic rats (Table 3).

Quantitative morphology in tibial nerve

Hypoglycemic animals (HI and HII). Also in the tibial nerve the caliber spectra of myelinated fibers were shifted toward smaller fiber sizes ($P < 0.001$) (Fig. 3a) which was associated with a 20% reduction in mean fiber size ($P < 0.0001$) (Table 4). These changes probably reflect Wallerian degeneration and loss of predominantly large myelinated fibers, whereas myelinated fibers of lesser size appeared to be relatively spared (Fig. 4). No changes were demonstrated in fiber densities, whereas fiber occupancies were significantly reduced when compared with age-matched control rats ($P < 0.02$ and $P < 0.001$ in HI and HII respectively compared to C in Table 4). This discordance in fiber density and occupancy probably reflects loss of large myelinated fibers which are partly replaced by small regenerating fibers (see column H in Table 5), and a noticeable endoneurial edema in hypoglycemic tibial nerves, further decreasing the already diminished occupancy by small regenerating fibers (Fig. 5). The axon–myelin ratios of tibial nerve fibers in hypoglycemic animals were markedly reduced compared with non-diabetic control animals ($P < 0.01$) (compare HI and HII with C in Fig. 2b) and were also reduced ($P < 0.05$) compared with hyperglycemic animals receiving no continuous insulin supplementation (DII in Fig. 2b). Thus the greater decrease in

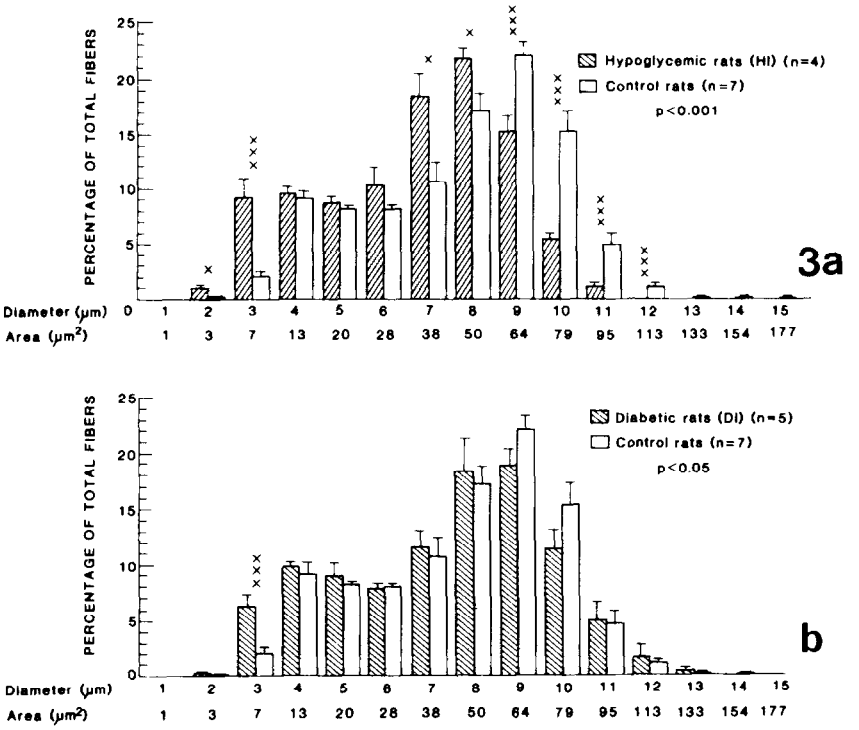

Fig. 3. Myelinated fiber size distributions in tibial nerves were calculated and constructed in the same way as for sural nerves. (a) Acutely hypoglycemic rats (HI) are compared with age- and sex-matched controls (C). Similar to the changes seen in the sural nerve, hypoglycemic rats exhibited marked decreases in the frequencies of large myelinated fibers, most likely representing loss of this fiber category. In addition, hypoglycemic rats showed a small increase in the smallest fibers, probably representing the addition of small newly regenerated myelinated fibers. (b) Myelinated fiber size distributions in insulin-treated diabetic rats (DI) and control rats (C) are compared. No significant differences are demonstrated, except for 3 μm fibers which are increased in diabetics, probably reflecting the significant increase in regenerating fibers (compare column H in Table 5).

myelinated fiber size in hypoglycemic rats compared with hyperglycemic animals (Table 4) may in part reflect a more severe axonal atrophy in the former groups.

Hyperglycemic animals (DI and DII). Only minimal shifts toward smaller fiber sizes were demonstrated in myelinated fiber caliber spectra of the tibial nerve (Fig. 3b). Mean myelinated fiber size was only moderately ($P < 0.02$) reduced in diabetic animals receiving insulin compared with age-matched control rats (compare DI with C in Table 4). However, the mean myelinated fiber size in hyperglycemic animals was greater than in both hypoglycemic groups (compare DI and DII with HI and HII in Table 4). No differences were demonstrated in fiber densities when compared with non-diabetic control rats or hypoglycemic rats (Table 4). Myelinated fiber occupancy was not reduced in diabetic rats receiving small maintenance doses of insulin, whereas those receiving no insulin showed a 20% reduction in fiber occupancy ($P < 0.02$) (Table 4). The moderate change in mean myelinated fiber size in the tibial nerve in hyperglycemic animals receiving insulin supplementation (Table 4) corresponded to a moderate decrease ($P < 0.02$) in the axon–myelin ratio (Fig. 2b), whereas diabetic animals receiving no insulin exhibited no significant change in the axon–myelin ratio (Fig. 2b).

Teased fiber analysis of tibial nerve

Hypoglycemic animals (HI and HII). The pattern of single teased fiber abnormalities in the tibial

TABLE 3

SCORED PATHOLOGY OF TEASED SURAL NERVE FIBERS

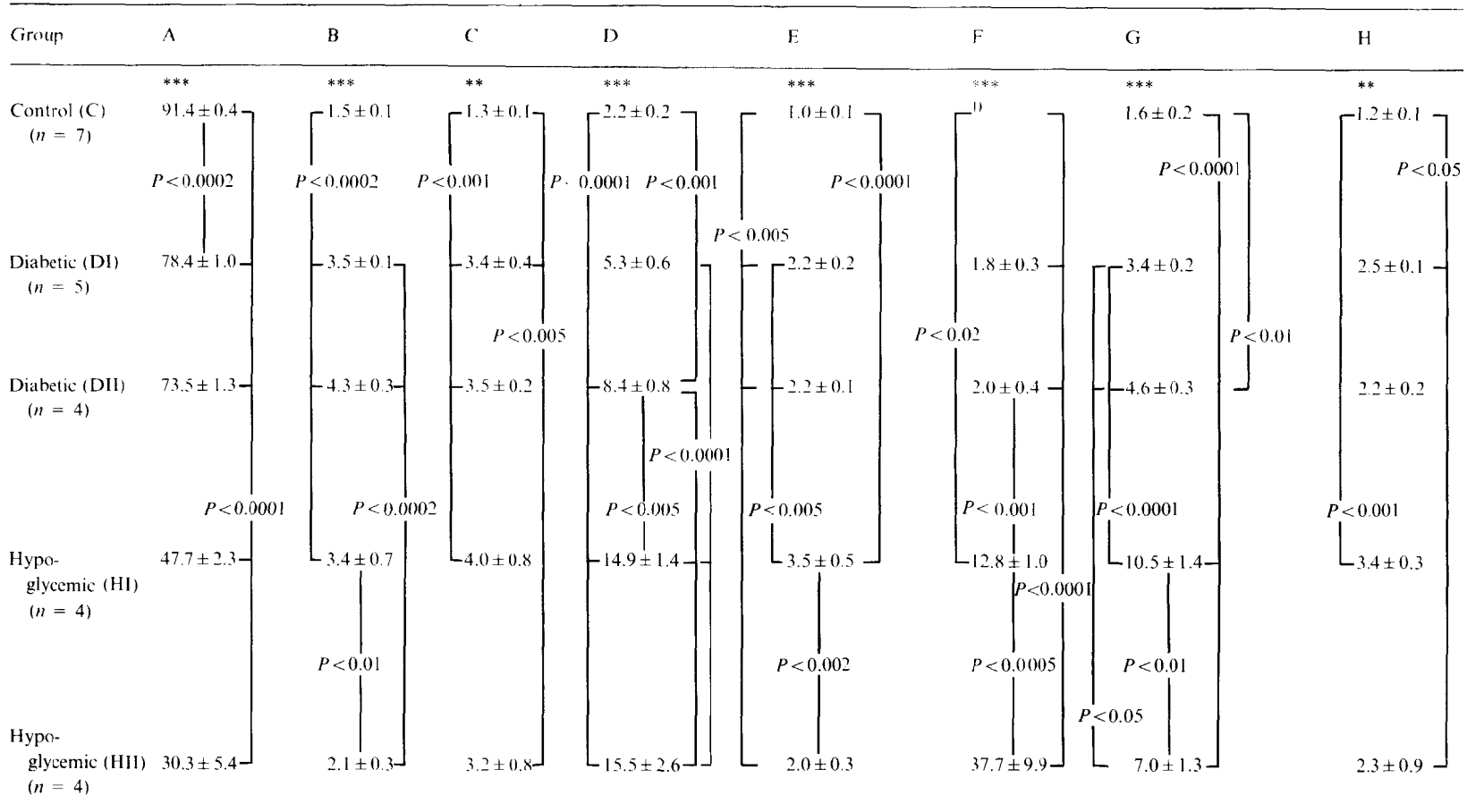

Scored pathology of single teased fibers expressed as mean (±SEM) percentages of total fibers. A, normality; B, paranodal swelling; C, paranodal demyelination; D, excessive myelin wrinkling; E, intercalated nodes; F, Wallerian degeneration; G, segmental demyelination; H, remyelinating or regenerating fibers. Diabetic rats (DI and DII) and hypoglycemic rats are compared with age-matched non-diabetes prone control rats (C).

*** ANOVA $P < 0.0001$.

** ANOVA $P < 0.001$.

TABLE 4

NUMERICAL MORPHOMETRIC DATA ON TIBIAL NERVES

	Mean fiber size (μm)	Fiber density (fibers/mm^2)	Fiber occupancy (%)
	**		*
Control (C) (n = 7)	50.5 ± 0.8	13318 ± 296	67.3 ± 1.7
	$P<0.02$		
	$P<0.0001$		
Diabetic (DI) (n = 5)	46.4 ± 1.7	14019 ± 672	64.7 ± 2.1
	$P<0.01$		$P<0.02$
Diabetic (DII) (n = 4)	47.5 ± 2.5	11621 ± 1670	54.0 ± 5.0
	$P<0.005$		$P<0.001$
Hypoglycemic (HI) (n = 4)	40.4 ± 1.0	13010 ± 819	53.4 ± 4.6
	$P<0.0005$		$P<0.005$
Hypoglycemic (HII) (n = 4)	38.3 ± 0.3	12348 ± 1611	47.5 ± 6.6

Mean myelinated fiber size, fiber density and fiber occupancy of tibial nerves are compared in diabetic, hypoglycemic and non-diabetes-prone control rats.

** ANOVA $P<0.0001$.

* ANOVA $P<0.005$.

nerve was similar to that in the sural nerve (Table 5). Excessive myelin wrinkling, characterizing axonal atrophy and Wallerian degeneration, was more frequent in tibial nerves from hypoglycemic animals killed 1 week after excessive insulin treatment (HII) (Fig. 4) than in those killed immediately following insulin treatment (HI) (Table 5).

Hyperglycemic animals (DI and DII). The frequency of single teased myelinated fiber abnormalities in tibial nerves of diabetic rats showed a similar distribution to that exhibited by sural nerves. The frequencies of fibers showing excessive myelin wrinkling and regenerating fibers appeared to be somewhat greater in the tibial nerve compared with the sural nerve (compare columns D and H in Table 5 with those in Table 3). Paranodal swelling was significantly ($P < 0.001$) more frequent in diabetic rats receiving no insulin supplementation than in hypoglycemic rats (Table 5).

Density of α motoneurons and dorsal root ganglion cells

Hypoglycemic animals (HI and HII). The density of α motoneurons of the L5 segment of the spinal

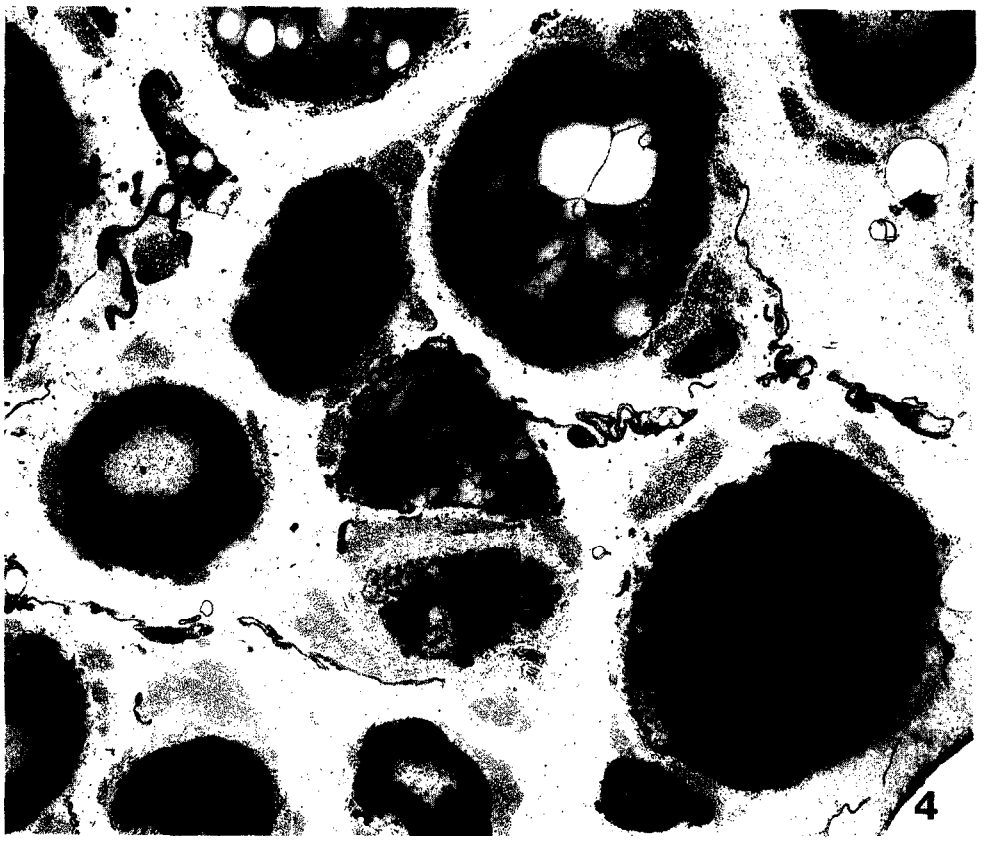

Fig. 4. Electron micrograph of the tibial nerve in an acutely hypoglycemic rat (HI). There are several large myelinated fibers showing various stages of Wallerian degeneration as well as smaller sized myelinated fibers showing axonal atrophy with wrinkling of the myelin sheaths. 4400 ×.

cord was reduced to approximately 60% of normal in both hypoglycemic groups ($P < 0.001$ and $P < 0.002$ for HI and HII respectively; Table 6). The loss of dorsal root ganglion cells, as reflected by their density, was less severe but increased following the discontinuation of excessive insulin treatment. In acutely hypoglycemic rats (HI) the density was reduced to 80% ($P < 0.05$) with a further reduction to 65% ($P < 0.001$) of normal 1 week following the period of hypoglycemia (HII) (Table 6).

Hyperglycemic animals (DI and DII). No significant loss of α motoneurons or dorsal root ganglion cells could be demonstrated in either diabetic group (DI and DII in Table 6).

Discussion

The diabetic neuropathy occurring in the spontaneously diabetic BB rat has previously been characterized as a mainly sensory distal axonopathy [16,17,20]. The present findings tend to confirm this, since myelinated fiber atrophy was more pronounced in the mainly sensory sural nerve than in the mixed sensory-motor tibial nerve. Diabetic animals failed in the present study to show any loss of sensory ganglion cells in the dorsal root ganglia or loss of α motoneurons in the anterior horn, suggesting that the axonopathy is not the consequence of an underlying neuronopathy.

Myelinated fiber atrophy occurring in diabetic

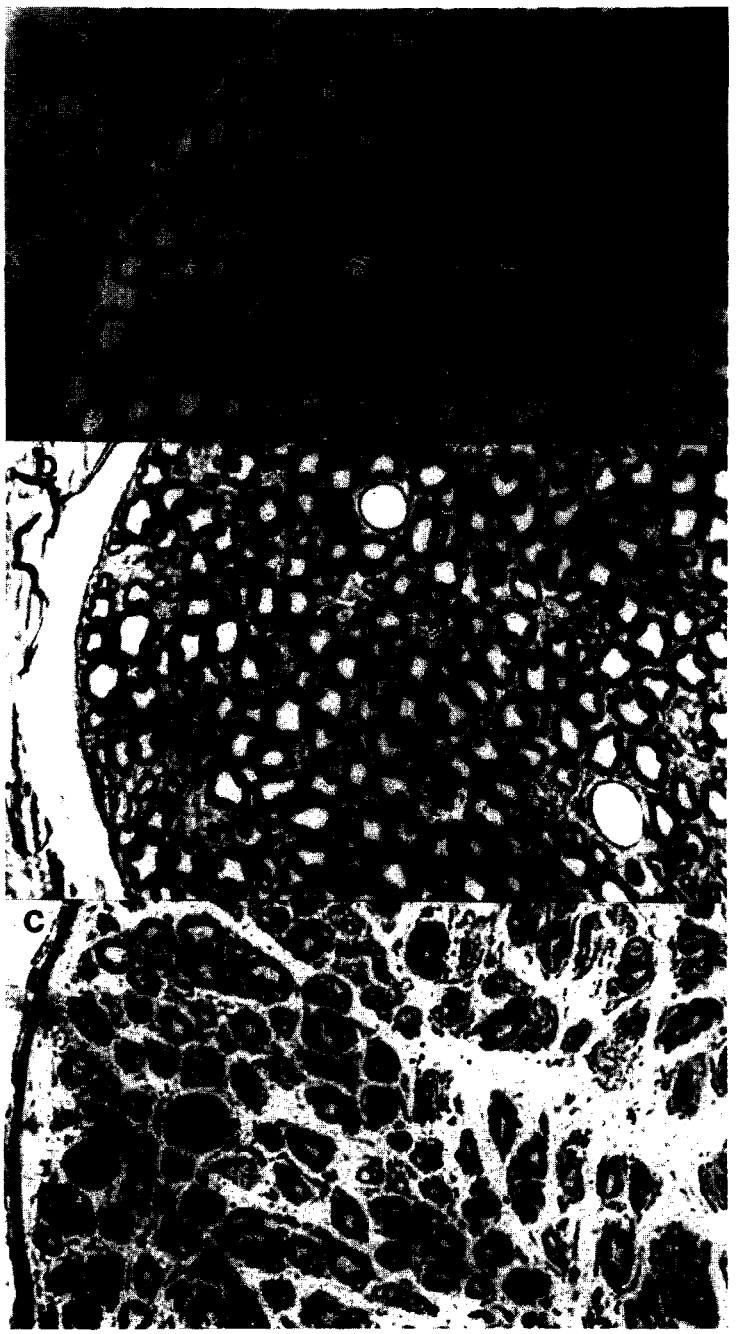

Fig. 5. Micrographs of tibial nerves in (a) a control rat; (b) non-insulin-treated diabetic rat (DII); and (c) hypoglycemic rat killed 1 week following hypoglycemia (HII). In b, axonal atrophy is evident by the irregular myelin sheaths. In c, there is marked loss of large myelinated fibers, some of which are still undergoing Wallerian degeneration (left part in c). In addition there is endoneurial edema, which in part may explain the discordance between fiber density and fiber occupancy in this hypoglycemic group (HII) (compare Table 4). 400 ×.

TABLE 5

SCORED PATHOLOGY OF TEASED TIBIAL FIBERS

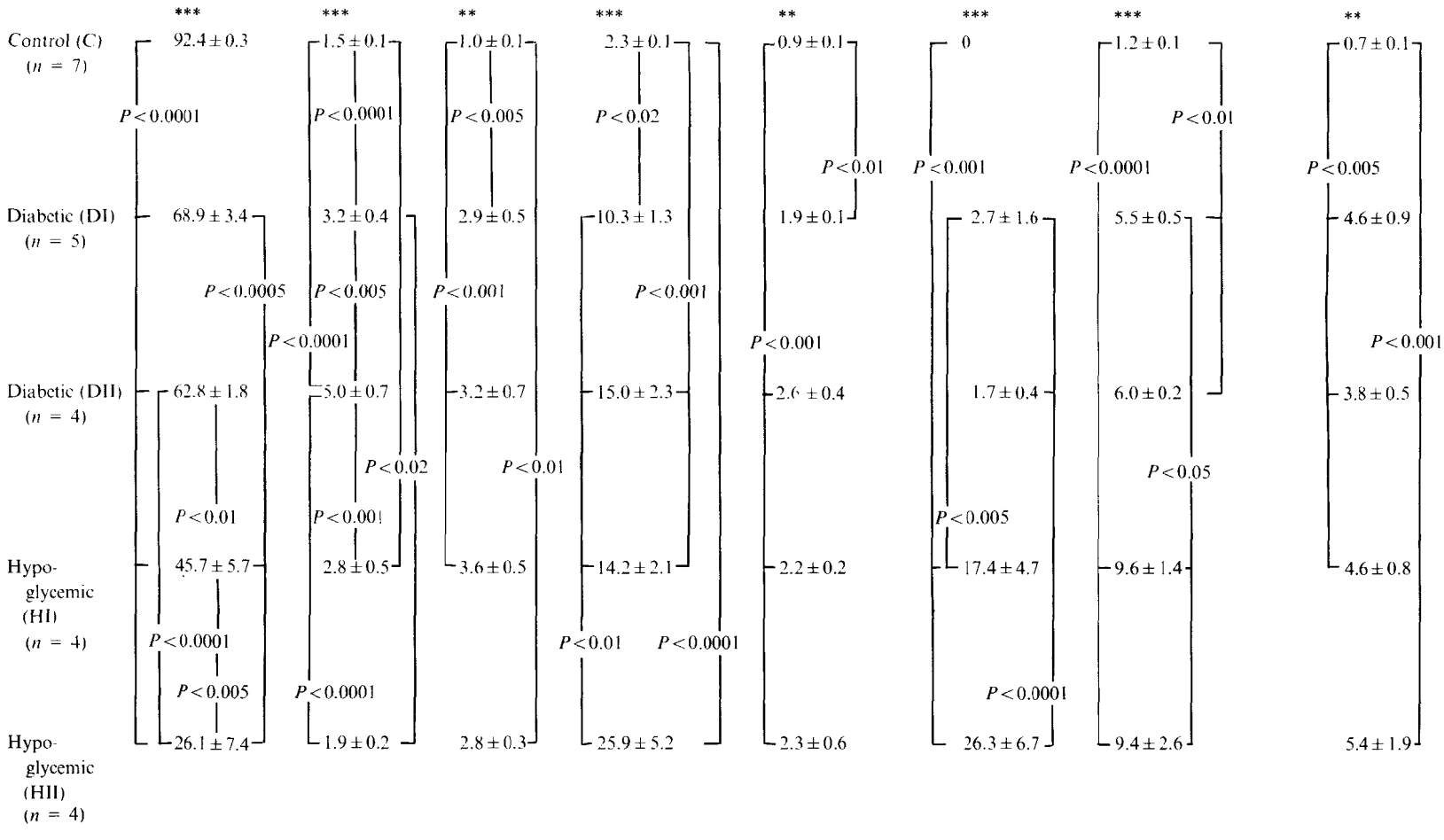

Scored pathology of single teased myelinated fibers expressed as mean (± SEM) percentages of total fibers. Diabetic rats (DI and DII) and hypoglycemic rats (HI and HII) are compared with non-diabetes-prone control rats (C).

*** ANOVA $P < 0.0001$.

** ANOVA $P < 0.001$.

TABLE 6

DENSITY OF ALPHA MOTONEURONS AND DORSAL ROOT GANGLION CELLS

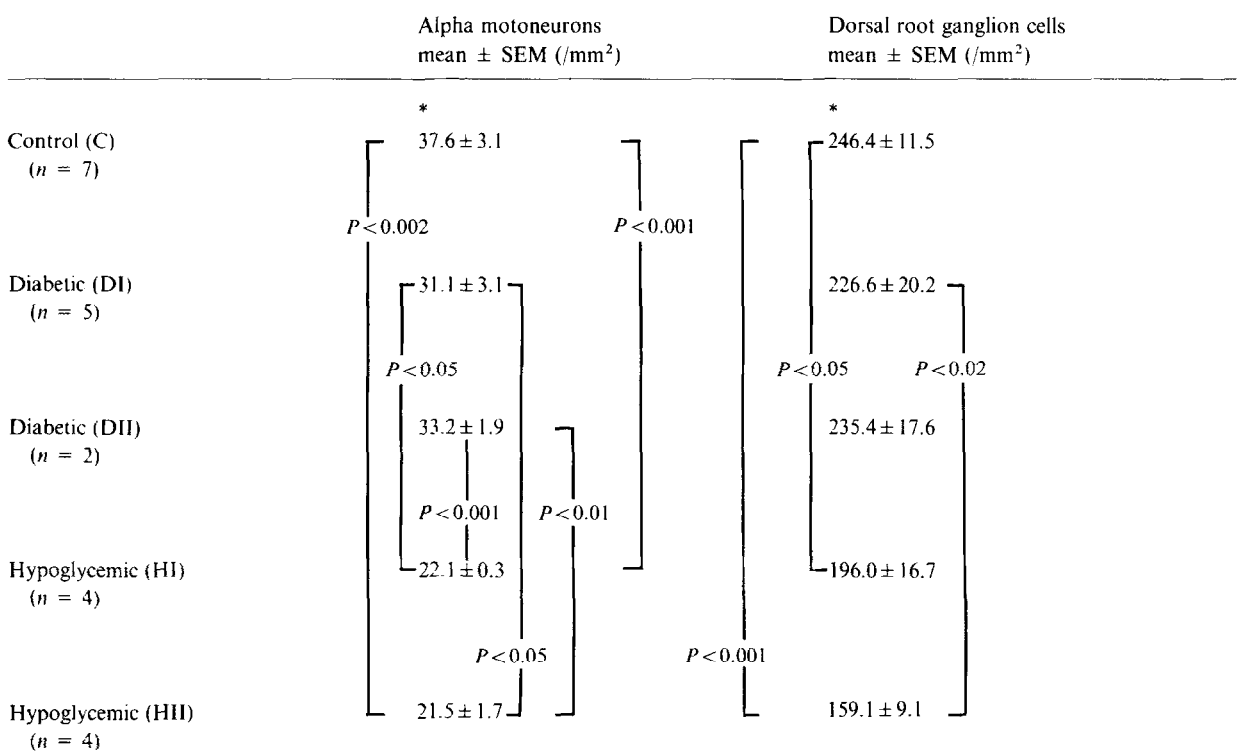

The density of α motor neurons of the L5 segment and dorsal root ganglion cells of L5 expressed as number of cells per mm^2 is compared in the various experimental groups.

* ANOVA $P<0.01$.

polyneuropathy appears to be primarily due to axonal atrophy as demonstrated by axon–myelin ratios and increased frequencies of fibers exhibiting excessive myelin wrinkling. As illustrated by these morphometric parameters, axonal atrophy appears to affect the mainly sensory sural nerve more severely than the mixed sensory-motor tibial nerve [16,30].

Additional structural abnormalities previously described in peripheral nerve of the diabetic BB rat and human diabetic neuropathy involve the node of Ranvier, such as nodal and/or paranodal axonal swelling, paranodal demyelination, and remyelination [9,12,13,18]. These findings were confirmed by the present teased fiber analysis.

Continuous supplementation of small insulin doses to diabetic BB rats did not have an additional deleterious effect on the severity of the neuropathy, nor did it seem to alter the nature of the neuropathy when compared with diabetic BB rats that did not receive exogenous insulin but were maintained at similar hyperglycemic levels throughout their course of diabetes. On the contrary, non-insulin-supplemented rats tended to develop a more severe expression of the characteristic structural abnormalities of diabetic neuropathy, such as paranodal swelling and excessive myelin wrinkling suggesting a small beneficiary effect of even small continuous insulin injections. These structural abnormalities in diabetic rats were paralleled by a similar decrease in motor nerve conduction velocity in the two diabetic groups.

Thus it is unlikely that the neuropathy develop-

ing in the spontaneously diabetic BB rat with exogenous insulin supplementation is a consequence of the usually necessary exogenous insulin treatment and/or its vehicle, as has been previously suggested [24,25].

In order to examine the possibility that previously reported morphological findings in insulin-treated diabetic rats [24,25] may have been misinterpreted and instead represent hypoglycemic peripheral nerve damage arising from even short periods of hypoglycemia [31,32], peripheral nerves were examined from two groups of BB rats exposed to hypoglycemia. The prevailing structural findings in these animals were Wallerian degeneration, segmental demyelination, and axonal atrophy which are in agreement with those previously reported in both experimental animals [31,32] and in man [33–35] consequent to hypoglycemia. They are similar to the findings reported in insulin-treated diabetic rats by Mandelbaum and collaborators [24,25] who demonstrated an eightfold increase in the frequency of fibers exhibiting Wallerian degeneration compared with non-insulin-treated diabetic rats.

The high frequencies of myelinated fibers exhibiting Wallerian degeneration in both the sural and tibial nerves corresponded to marked losses of dorsal root ganglion cells and anterior horn α motoneurons, abnormalities which were not demonstrable in diabetic rats. These findings, therefore, confirm that prolonged severe hypoglycemia affects primarily the cell bodies with subsequent Wallerian degeneration [31,32,35].

In contrast to diabetic neuropathy which involves mainly sensory fibers, hypoglycemic neuropathy appears to affect motor fibers more severely as reflected by a larger loss of motoneurons compared to sensory neurons, and by a more severe reduction in mean fiber size in the sensory-motor tibial nerve compared with the mainly sensory sural nerve. The increased vulnerability of motoneurons versus sensory ganglion cells in hypoglycemic BB rats appears to be similar to the situation in man as reflected by clinical findings and electrophysiologic deficits reported in a few patients with hypoglycemia [34,36–39]. In addition to the acute effect of glucopenia on motoneurons, a prolonged and progressive adverse effect on nerve morphology was evident following discontinuation of hypoglycemic exposure with an accentuation of Wallerian degeneration and axonal atrophy.

In summary therefore, it is unlikely that continuous small insulin dosing in the spontaneously diabetic BB rat has any etiological relevance with respect to the development of diabetic neuropathy in this model. In contrast, it may have a marginally beneficiary effect on this complication despite the fact that the rats are maintained at severely hyperglycemic levels. Hypoglycemia in the same model causes an acute and progressive severe neuropathy resulting in neurological deficits and slowing of MNCV. In contrast to diabetic neuropathy, hypoglycemic nerve damage tends to affect motor fibers more than sensory fibers and might be characterized as a neuronopathy rather than an axonopathy.

Acknowledgements

This study was supported in part by grants from the JDFI, New York, NY, and from the Medical Research Council of Canada (MA-8681 and MA-9351). The authors are indebted to Mrs. Jackie McKane for preparing the manuscript.

References

1 Behse, F., Buchtal, F. and Carlson, F. (1977) Nerve biopsy and conduction studies in diabetic neuropathy. J. Neurol. Neurosurg. Psychiatry 40, 1072–1082.

2 Hansen, S. and Ballantyne, J.P. (1977) Axonal dysfunction in the neuropathy of diabetes mellitus: a quantitative electrophysiological study. J. Neurol. Neurosurg. Psychiatry 40, 555–564.

3 Bischoff, A. (1973) Ultrastructural pathology of peripheral nervous system in early diabetes. In: R.A. Camerini-Davalos and H.S. Cole (Eds.), Vascular and Neurologic Changes in Early Diabetes. Academic Press, New York, NY, pp. 441–449.

4 Said, G., Slama, G. and Selva, J. (1983) Progressive centripetal degeneration of axons in small fiber diabetic polyneuropathy. Brain 106, 791–807.

5 Dyck, P.J., Lais, A., Karnes, J.L., O'Brien, P. and Rizza, R. (1986) Fiber loss in primary and multifocal sural nerves in diabetic polyneuropathy. Ann. Neurol. 19, 425–439.

6 Dyck, P.J., Karnes, J.L., O'Brien, P., Okazaki, H., Lais, A. and Engelstad, J. (1986) The spatial distribution of fiber loss in diabetic polyneuropathy suggests ischemia. Ann. Neurol. 19, 440–449.

7 Johnson, P.C., Doll, S.C. and Cromey, D.W. (1986) Pathogenesis of diabetic neuropathy. Ann. Neurol. 19, 450–457.

8 Dyck, P.J., Karnes, J., Lais, A., Lofgren, E.P. and Stevens, J.C. (1984) Pathologic alterations of the peripheral nervous system of humans. In: P.J. Dyck, P.K. Thomas, E.H. Lambert and R. Bunge (Eds.), W.B. Saunders, Philadelphia, PA, pp. 760–870.

9 Sima, A.A.F., Nathaniel, V., Bril, V., McEwen, T.A.J. and Greene, D.A. (1988) Histopathological heterogeneity of neuropathy in insulin-dependent and non-insulin-dependent diabetes, and demonstration of axo-glial dysjunction in human diabetic neuropathy. J. Clin. Invest. 81, 349–364.

10 Greene, D.A., Chakrabarti, S., Lattimer, S.A. and Sima, A.A.F. (1987) Role of sorbitol accumulation and *myo*-inositol depletion in paranodal swelling of large myelinated nerve fibers in the insulin deficient spontaneously diabetic Bio-breeding rat: reversal by insulin replacement, an aldose reductase inhibitor and *myo*-inositol. J. Clin. Invest. 79, 1479–1485.

11 Brismar, T. and Sima, A.A.F. (1981) Changes in nodal function in nerve fibers of the spontaneously diabetic BB-Wistar rat. Potential clamp analysis. Acta Physiol. Scand. 113, 499–506.

12 Sima, A.A.F. and Brismar, T. (1985) Reversible diabetic nerve dysfunction: structural correlates to electrophysiological abnormalities. Ann. Neurol. 18, 21–29.

13 Brismar, T., Sima, A.A.F. and Greene, D.A. (1987) Reversible and irreversible nodal dysfunction in diabetic neuropathy. Ann. Neurol. 21, 504–507.

14 Chakrabarti, S., Sima, A.A.F., Nakajima, S., Yagihashi, S. and Greene, D.A. (1987) Aldose reductase in the BB-rat: isolation, immunological identification and localization in the retinal and peripheral nerve. Diabetologia 30, 244–251.

15 Sima, A.A.F. (1980) Peripheral neuropathy in the spontaneously diabetic BB-Wistar rat. Acta Neuropathol. 51, 223–232.

16 Sima, A.A.F., Bouchier, M. and Christensen, H. (1983) Axonal atrophy in sensory nerves of the diabetic BB-Wistar rat. A possible early correlate of human diabetic neuropathy. Ann. Neurol. 13, 264–272.

17 Sima, A.A.F. (1985) Annotation: Can the BB-rat help to unravel diabetic neuropathy? Neuropathol. Appl. Neurobiol. 11, 253–264.

18 Sima, A.A.F., Lattimer, S.A., Yagihashi, S. and Greene, D.A. (1986) Axo-glial dysfunction. A novel structural lesion that accounts for poorly reversible slowing of nerve conduction in the spontaneously diabetic Bio-breeding rat. J. Clin. Invest. 77, 474–484.

19 Sima, A.A.F. and Thibert, P. (1982) Proximal motor neuropathy in the BB-Wistar rat. Diabetes 31, 784–788.

20 Sima, A.A.F. and Yagihashi, S. (1986) Distal central-peripheral axonopathy in the spontaneously diabetic BB-Wistar rat: an ultrastructural and morphometric study. Diabetes Res. Clin. Pract. 1, 289–298.

21 Greene, D.A., Yagihashi, S., Lattimer, S.A. and Sima, A.A.F. (1984) Nerve Na^+-K^+-ATPase, conduction and myo-inositol in the insulin deficient BB-rat. Am. J. Physiol. 247, E534–E539.

22 Greene, D.A., Lattimer, S.A. and Sima, A.A.F. (1987) Sorbitol, phosphoinositides and the sodium-potassium ATPase in the pathogenesis of diabetic complications. N. Engl. J. Med. 316, 599–606.

23 Sima, A.A.F., Brismar, T. and Yagihashi, S. (1987) Neuropathies encountered in the spontaneously diabetic BB Wistar rat. In: P. Dyck, P.K. Thomas, A.K. Asbury, A.I. Winegrad and D. Porte Jr. (Eds.), Diabetic Neuropathy. W.B. Saunders, Philadelphia, PA, pp. 253–259.

24 Westfall, S.G., Felten, D.L., Mandelbaum, J.A., Moore, S.A. and Peterson, R.G. (1983) Degenerative neuropathy in insulin-treated diabetic rats. J. Neurol. Sci. 61, 93–107.

25 Mandelbaum, J.A., Felten, D.L., Westfall, S.G., Newlin, G.E. and Peterson, R.G. (1983) Neuropathic changes associated with insulin treatment of diabetic rats: electronmiscroscopic and morphometric analysis. Brain Res. Bull. 10, 377–384.

26 Marliss, E.B., Sima, A.A.F. and Nakhooda, A.F. (1981) Spontaneous diabetes in the 'BB' Wistar rat. In: J.M. Martin et al. (Eds.), Etiology and Pathogenesis of Insulin-Dependent Diabetes Mellitus. Raven Press, New York, NY, pp. 251–274.

27 Marliss, E.B., Nakhooda, A.F., Poussier, P. and Sima, A.A.F. (1982) The diabetic syndrome of the BB Wistar rat. Possible relevance to type I (insulin-dependent) diabetes in man. Diabetologia 22, 225–232.

28 Sima, A.A.F. and Hay, K. (1981) Functional aspects and pathogenetic considerations of the neuropathy in the spontaneously diabetic BB-Wistar rat. Neuropathol. Appl. Neurobiol. 7, 341–350.

29 Dyck, P.J., Karnes, J., Lais, A., Lofgren, E.P. and Stevens, J.C. (1984) Pathologic alterations of the peripheal nervous system of humans. In: P.J. Dyck, P.K. Thomas, E.H. Lambert and R. Bunge (Eds.), Peripheral Neuropathy. W.B. Saunders, Philadelphia, PA, pp. 760–870.

30 Mendell, J.R., Sahenk, Z., Wormolts, J.R., Marshall, J.K. and Thibert, P. (1981) The spontaneously diabetic Wistar rat. Morphologic and physiologic studies of peripheral nerve. J. Neurol. Sci. 52, 103–115.

31 Sidenius, P. and Jakobsen, J. (1983) Peripheral neuropathy in rats induced by insulin treatment. Diabetes 32, 383–386.

32 Jakobsen, J. and Sidenius, P. (1987) Hypoglycemic neuropathy. In: P. Dyck, P.K. Thomas, A.K. Asbury, A.I. Winegrad and D. Porte Jr. (Eds.), Diabetic Neuropathy. W.B. Saunders, Philadelphia, PA, pp. 94–99.

33 Moersch, F.P. and Kernahan, J.W. (1938) Hypoglycemia: neurologic and neuropathologic studies. Arch. Neurol. Psychiatry 39, 242–257.

34 Tom, M.I. and Richardson, J.C. (1951) Hypoglycemia from islet cell tumor of pancreas with amyotrophy and cerebrospinal nerve cell damage. J. Neuropathol. Exp. Neurol. 10, 57–66.
35 Rosner, L. and Elstad, R. (1964) The neuropathy of hypoglycemia. Neurology 14, 1–6.
36 Danta, G. (1969) Hypoglycemic peripheral neuropathy. Arch. Neurol. 21, 121–132.
37 Harrison, M.J.G. (1976) Muscle wasting after prolonged hypoglycemic coma: case report with electrophysiological data. J. Neurol. Neurosurg. Psychiatry 39, 465–470.
38 Jaspan, J.B., Wollman, R.L., Bernstein, L. and Rubinstein, A.H. (1982) Hypoglycemic peripheral neuropathy in association with insulinoma: implication of glucopenia rather than hyperinsulinemia. Case report and literature review. Medicine 61, 33–44.
39 Editorial (1982) Hypoglycemic peripheral neuropathy. Lancet 2, 1447–1448.